SIAM J. Scientific Computing, 18, 239-256, 1997
sub. 5/1995, to appear SIAM J. Scientific Computing

THE ADAPTIVE VERLET METHOD

WEIZHANG HUANG† AND BENEDICT LEIMKUHLER‡

Abstract. We discuss the integration of autonomous Hamiltonian systems via dynamical rescaling of the vector field (reparameterization of time). Appropriate rescalings (e.g. based on normalization of the vector field or on minimum particle separation in an N-body problem) do not alter the time-reversal symmetry of the flow, and it is desirable to maintain this symmetry under discretization. For standard form mechanical systems without rescaling, this can be achieved by using the explicit leapfrog/Verlet method; we show that explicit time-reversible integration of the reparameterized equations is also possible if the parameterization depends on positions or velocities only. For general rescalings, a scalar nonlinear equation must be solved at each step, but only one force evaluation is needed. The new method also conserves the angular momentum for an N-body problem. The use of reversible schemes together with a step control based on normalization of the vector field (arclength reparameterization) is demonstrated in several numerical experiments, including a double pendulum, the Kepler problem and a three-body problem.

Key words. time-reversible methods, symplectic methods, Hamiltonian systems, variable stepsize methods, Verlet, leapfrog, N-body problems

1. Introduction. In this article we consider the numerical integration of autonomous differential equations in $\mathbf{R}^N$

$$\frac{d}{dt}u = f(u), \tag{1.1}$$

such as arise in celestial mechanics [22], (classical) atomic and molecular dynamics [12], and in many other important theoretical and practical situations. Direct integration (or simulation) is the principal tool for the study of such problems. Fixed stepsize numerical integration of nonlinear systems (1.1) leads to difficulties, particularly in the neighborhood of singularities of the vector field. This article describes a family of efficient adaptive methods for the numerical solution of initial value problems for equation (1.1) based on normalization of (or other dynamical scaling of) the vector field.

Recent research [17], [14], [10] has focused on the development of time-stepping schemes that preserve the underlying geometrical structure of the flow of the system (e.g. symplecticness in the case of Hamiltonian systems). Regardless of whether a scheme faithfully preserves available underlying structure, accurate and stable fixed stepsize numerical integration often requires excessively small timesteps. This is particularly true when integrating in the vicinity of fixed points and singularities. In principle, it is possible to incorporate stepsize variation mechanisms based on local error estimates, but many of the advantages of the structure-preserving schemes appear to be lost if the stepsize is varied using traditional approaches [4, 3, 7].

We consider an approach based on introduction of a time reparameterization. Given an appropriate smooth, scalar-valued function $R = R(u)$ with $0 < m < R < M$ for some m, M, we integrate the differential equations

$$\frac{d}{ds}u = \frac{f(u)}{R(u)}, \qquad \frac{dt}{ds} = \frac{1}{R(u)}. \tag{1.2}$$

† Department of Mathematics, the University of Kansas, Lawrence, KS 66045, U.S.A. (whuang@math.ukans.edu). Supported in part by NSF EPSCoR grant no. OSR-9255223.

‡ Department of Mathematics, the University of Kansas, Lawrence, KS 66045, U.S.A. (leimkuhl@math.ukans.edu). Supported by NSF grant no. NSF-9303223.

The behavior of trajectories in extended phase space will be highly sensitive to such reparameterizations, but in terms of the phase space orbits, the reparameterization is irrelevant. The flow of (1.2) preserves all integral invariants of (1.1). Once the flow has been reparameterized, (1.2) can be integrated by an appropriate fixed-stepsize discretization scheme.

A natural choice of R is given by the heuristic $R = \|f\|$, with $\|.\|$ the Euclidean 2-norm. The choice of such a normalization of the vector field can also be viewed as associating steps in time directly with steps in arclength measured along phase space orbits. This is not the only choice. Indeed, variants of this reparameterization idea have been used in various applications, for example basing R on the separation between particles in a many-particle system with a singular potential [1, 13, 11]. The techniques of [3, 21] can be viewed in this framework, where R is constructed based on an embedded local error estimate. Other heuristics would retain approximate constant arclength of some projection of the solution. A more accurate (and complicated) control could incorporate an estimate for the orbit curvature at a point. Some related recent work [18, 19] has used the reparameterization framework to design schemes that better conserve various integrals such as the energy.

We are particularly interested in systems based on a separated Hamiltonian $H(p,q) = \frac{1}{2}p^t M^{-1} p + V(q)$:

$$\dot{q} = M^{-1}p, \tag{1.3}$$

$$\dot{p} = -\nabla V. \tag{1.4}$$

It is well known that for large systems of types (1.3)-(1.4) such as one encounters in molecular dynamics, the computational cost of simulation is dominated by force evaluations. These problems are often solved by the explicit leapfrog (Verlet) method which is second order, symplectic, time-reversible (symmetric), and requires only one force evaluation per step. For large N-body problems, much recent work has concentrated on finding methods to handle singularities or widely varying forces without having to evaluate the full force field at every integration step. By basing these methods on potential-specific splittings, they can sometimes achieve the effect of a variable stepsize method (see [20]). This article takes a different approach in rather trying to adapt the time stepsize directly according to some prescribed rescaling of time.

For (1.3)-(1.4), using $R = \|f\|$ corresponds to reparameterization based on the norm of the gradient of the Hamiltonian, hence according to the density of flow lines along the solution. In general, reparameterization of (1.3)-(1.4) will destroy the Hamiltonian structure, but time-reversibility of the flow is easily preserved. The coupling structure of (1.3)-(1.4) is altered by reparameterization, and the natural generalization of the leapfrog/Verlet scheme (which retains such features as conservation of angular momentum and time-reversibility) becomes implicit. For example, the schemes of [21, 3, 11] all lead to implicit integration strategies requiring the evaluation of forces $-\nabla V$ *several times per integration step*. The main practical contribution of this article is to show that this implicitness can be removed by the use of a special discretization method that treats the reparameterization factor as a new variable to be propagated together with the physical variables. We call this new method *Adaptive Verlet*.

Actually, we discuss two variants of the method: one based on differentiation of the equation defining the reparameterization factor, and the other based on introduction of an algebraic equation which is then solved in tandem with the equations of motion by use of an ad hoc discretization scheme. This latter differential-algebraic approach requires no additional force evaluations at a step and it is our recommended

method for typical applications. We stress that for reparameterizations depending on p and q such as that based on arclength, the additional work of the Adaptive Verlet method over standard Verlet consists only of the solution of a single scalar quartic polynomial equation at each timestep. Such an efficient implementation would also be possible for many other choices of the rescaling; in fact, for the special case *where the rescaling is based on either positions or momenta only, the equations become fully explicit.* Control of minimum and maximum stepsizes is also easily incorporated in our framework.

The methods are implemented for various simple nonlinear models which are meant to be representative of typical autonomous systems: a double pendulum, the Kepler problem, and a three-body problem and are found to be robust and efficient in our experiments.

2. Background. For smooth f, the initial value problem (1.1), $u(t_0) = u_0$ has at least a local solution through any given u_0; we will assume that these solutions exist for all time. Associated with (1.1) is thus a *flow-map* $\phi[t_0, t_1]$ which takes a given point $u \in \mathbf{R}^N$ to the point $u_* = u(t_1)$ where $u(t)$ is the solution of (1.1), $u(t_0) = u_0$. The (forward) *trajectory* passing through a given point (t_0, u_0) is the set $\{(t, \phi[t_0, t](u_0)) | 0 \leq t < \infty\}$.

There are two ways in which trajectories are unnatural for describing the solutions of autonomous differential equations. First, because (1.1) is autonomous, it follows that $\phi[t_0, t](u_0) = \phi[0, t - t_0](u_0)$. (In the sequel, we will write $\phi[t]$ for $\phi[0, t]$.) This means that the inclusion of the initial time t_0 in the description of solutions is inherently arbitrary. Second, if we rescale the vector field solving instead

$$\frac{d}{dt}u = cf(u)$$

the solution u is unchanged except for a rescaling of time. For these reasons, it is generally more natural to replace the trajectory through u_0 by the *orbit* of u_0 defined as the set $\{\phi[t](u_0) | -\infty \leq t < \infty\}$. The orbits are scale and translation invariant.

A one-step method for solving (1.1) is a computable approximation to the flow map, i.e. it is a map $\psi[\Delta t]$ of $\mathbf{R}^N$ such that $\|\psi[\Delta t](u_0) - \phi[\Delta t](u_0)\| \to 0$ as $\Delta t \to 0$. For a given stepsize Δt, the numerical (forward) orbit of a point u_0 is the discrete set $\{u_0, \psi[\Delta t](u_0), \psi[\Delta t]^2(u_0), \ldots\}$. The method is said to be pth order accurate if

$$\max_{n=0,1,\ldots N} \|\psi[\Delta t]^n(u_0) - \phi[n\Delta t](u_0)\| \leq K\Delta t^p,$$

where $N\Delta t = T$ is fixed and $K > 0$ is independent of Δt.

The implicit midpoint method defined for (1.1) by

$$u_{n+1} = u_n + \Delta t f(\frac{u_n + u_{n+1}}{2})$$

is a second order accurate scheme. A popular method for integrating the separable system (1.3)-(1.4) is the leapfrog/Verlet scheme:

$$\begin{aligned} q_{n+1} &= q_n + \Delta t M^{-1} p_{n+\frac{1}{2}}, \\ p_{n+\frac{1}{2}} &= p_n - \frac{\Delta t}{2}\nabla V(q_n), \\ p_{n+1} &= p_{n+\frac{1}{2}} - \frac{\Delta t}{2}\nabla V(q_{n+1}). \end{aligned}$$

This scheme is explicit, requires only one force evaluation per step, and is 2nd order accurate.

For the Hamiltonian system (1.3)-(1.4), *time-reversibility* of the flow is a consequence of the fact that $T(p) = \frac{1}{2}p^t M^{-1} p$ is an even function. This means that integrating (1.3)-(1.4) from some starting point Δt units forward in time, then changing the sign of the momentum and integrating another Δt units returns us to the starting position. The flow map is also *symplectic*, meaning that the two form $dq \wedge dp$ is an integral of motion [6, 17]. These geometric symmetries (symplecticness, time-reversal symmetry) impose strong restrictions on the possible types of fixed points and on the stability of motion in the neighborhood of fixed points.

Recent research on timestepping schemes has concentrated on finding numerical methods $\psi[\Delta t]$ which share the time-reversibility and/or symplecticness of the flow. For example, both the leapfrog and implicit midpoint methods are time-reversible. They are also both symplectic [6, 16]. The implicit midpoint method (and its Gauss-Legendre generalizations) preserves all quadratic integral invariants [5], while the leapfrog scheme (and the broader family of Lobatto IIIa-b pair Partitioned Runge-Kutta methods) can be shown to preserve the angular momentum [17]. When a constant stepsize is used, these methods both show remarkable long term stability with respect to energy error, except in the presence of large forces.

Symplectic (or time-reversible) methods exhibit linear error growth in periodic or integrable cases [3]. The composition of any two symplectic (time-reversible) maps is again symplectic (time-reversible), so it is natural to consider varying the stepsize from step to step. Stepsize selection strategies add a layer of complexity to the discrete dynamical system, since the stepsize then becomes a function of the dynamic variables [7]. Experiments with standard variable stepsize integration heuristics have been disappointing, for example, the general stability of energy and the linear growth of errors for integrable systems are lost [16, 3]. Time-reversible variable stepsize methods used in conjunction with underlying symplectic schemes as considered by Calvo and Hairer [3] have been observed to recapture some of the favorable features of symplectic/reversible schemes. In this article, we are mainly concerned with the treatment of generic (nonintegrable) dynamics, but we also observed the linear growth of errors of [3] for the Kepler problem with our reversible scheme.

3. Singularities and normalization of the vector field. The interactions of a pair of bodies under a Coulomb potential ($V = -1/r$, where r is the distance between the particles) can be regularized by introduction of a new coordinate system which removes the singularity. In the N-body problem, the two-body interactions can be similarly regularized [1, 13, 15] but the singularity representing the collision of three or more particles cannot be eliminated. Similar problems arise with other singular potentials. This means that some sort of timestep contraction is needed in the neighborhood of the singularities in order to resolve the behavior accurately. Even without singularities, it is unlikely that a single, fixed timestep will be appropriate along a whole orbit.

An insight into the selection of timestep is obtained by noting that for many problems the norm of the gradient of the Hamiltonian (and hence the norm of the vector field) is large at the places where the time scale changes rapidly and the fixed stepsize integrator performs poorly. The norm of the gradient of H measures the fastest directed rate of change of the Hamiltonian, hence the fixed stepsize integrators appear to fail at points where many orbits get "squeezed together." To put it another way, the fixed stepsize integrator may develop instabilities at points where the density

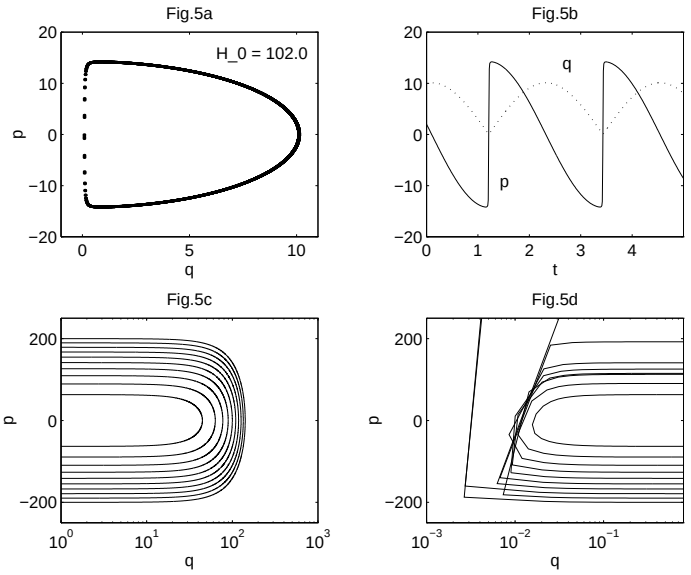

FIG. 1. *Fixed stepsize Verlet method for problem (3.5) with* $t_f = 50$ *and* $\Delta t = 0.0001$.

of flowlines of the system is large.

As an example of a simple singularity system, we consider the "bond problem" with Hamiltonian

$$H = \frac{1}{2}p^2 + \frac{1}{2q^2} + q^2. \tag{3.5}$$

The orbits of this system in phase space consist of two lobes of closed curves separated by the line $q = 0$. A sample orbit is shown in Fig. 1a. Although this orbit is quite smooth, the timescale changes dramatically in the neighborhood of the origin and the path from the lower left extreme point on the orbit to the upper left point is traversed extremely rapidly. In Fig. 1b, this rapid variation appears as an exceptionally steep derivative of p.

We applied the fixed-stepsize Verlet scheme to integrate the bond problem and the results for several orbits are shown in Figs. 1c-d with a single fixed stepsize $\Delta t = 0.0001$. The integration proceeds without difficulty, even for very high energy levels, as long as the particle stays roughly to the right of the vertical line passing through the fixed point $q = 2^{-1/4}$. Nearer the origin, the curves break-up at relatively low energy levels and the integrator becomes unstable (Fig. 1d).

Another type of difficulty occurs when the equations of motion possess isolated near-singular points such as in the double pendulum with very unequal masses. In this case, cusp-like turning points appear in the solution which can create difficulties for fixed stepsize integrators. Although a diagonal rescaling (weighting) of the variables can sometimes remove the near-singular behavior, this is not generically feasible for complicated problems, so some mechanism is needed to improve the situation.

Now consider a local reparameterization of time according to (1.2) with $R(u) = ||f(u)||$. This normalizes the vector field and can be viewed as a control of the arclength measured along phase space orbits traversed per unit time. A similar heuristic $R(u) = \sqrt{1 + ||f(u)||^2}$ can be viewed as normalizing the arclength traversed along a trajectory

per unit time.

Although this article focuses on vector field normalization, the method could be applied to work with many other choices of R. For example, for particle motion in central forces, we may typically assume that the closest two-body approach determines the largest force in the problem. We can introduce the control $R = 1/r_{\min}^{\alpha}$, where $r_{\min}$ represents the smallest interparticle separation and α is a positive constant. This idea is suggested in [1, 13, 15, 11].

For the normalized vector field, it is reasonable to use a fixed stepsize integration, however, it is sometimes necessary to limit the variation of R to avoid excessively small steps in the neighborhood of singular points. It is easy to incorporate a maximum and minimum stepsize. For example, for $0 < m << 1 << M$, let

$$R(u) = \frac{\sqrt{||f(u)||^2 + m^2}}{\frac{1}{M}\sqrt{||f(u)||^2 + m^2} + 1}.$$

Given a minimum time stepsize $\Delta t_{\min}$ and a maximum time stepsize $\Delta t_{\max}$, and fictive timestep Δs, we set $m = \Delta s/\Delta t_{\max}$ and $M = \Delta s/\Delta t_{\min}$, then we have that

$$m \approx \frac{1}{\frac{1}{M} + \frac{1}{m}} < R(u) < M.$$

so Δt will be bounded between about $\Delta t_{\min}$ and $\Delta t_{\max}$.

One drawback of the normalization which becomes evident in the case of separated Hamiltonians (1.3)-(1.4) is that the normalized vector field is not separable. This means that explicit schemes, particularly leapfrog/Verlet, cannot be directly applied. In the next section, we will show how the Verlet method can be modified to provide an efficient semi-explicit approach to variable stepsize integration. Below, we first show the effectiveness of combining reparameterization and time-reversible integration procedures with an example.

Example 3.1: the double pendulum We consider the double pendulum problem with Hamiltonian

$$\begin{aligned} H = \quad & \frac{1}{2}(m_1 + m_2)\,\dot{\theta_1}^2 + m_2\dot{\theta_1}\dot{\theta_2}cos\alpha \\ & + \frac{1}{2}m_2\dot{\theta_2}^2 - (m_1 + m_2)gcos\theta_1 - m_2 gcos\theta_2, \end{aligned} \tag{3.6}$$

where $\alpha = \theta_1 - \theta_2$, g is the gravity constant, m_1 and m_2 are the masses, and the positions of the bobs are related to θ_1 and θ_2 by

$$\begin{aligned} x_1 &= sin\theta_1, & y_1 &= -cos\theta_1, \\ x_2 &= sin\theta_1 + sin\theta_2, & y_2 &= -cos\theta_1 - cos\theta_2. \end{aligned}$$

The equations of motion are

$$\begin{aligned} (m_1 + m_2)\ddot{\theta_1} + m_2\left(\ddot{\theta_2}cos\alpha + \dot{\theta_2}^2 sin\alpha\right) + (m_1 + m_2)\,gsin\theta_1 &= 0, \\ \ddot{\theta_1}cos\alpha + \ddot{\theta_2} - \dot{\theta_1}^2 sin\alpha + gsin\theta_2 &= 0. \end{aligned}$$

To make the problem challenging, we gave the two bobs very different masses ($m_1 << m_2$).

Because the Hamiltonian is nonseparable, we used the symplectic, time-reversible implicit midpoint method. A fixed step size method has little difficulty in resolving

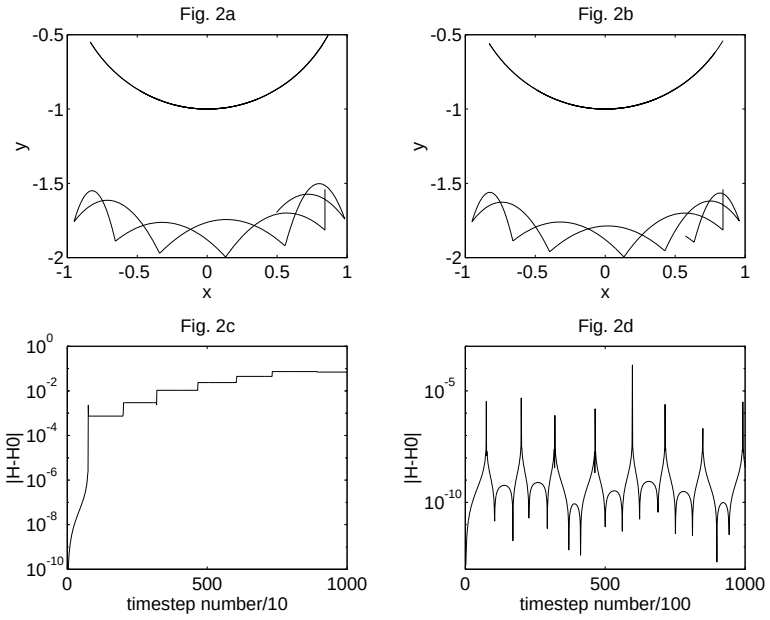

FIG. 2. *The implicit midpoint scheme with fixed stepsize for the double pendulum problem.* $(\theta_1^0, \theta_2^0, \dot{\theta_1}^0, \dot{\theta_2}^0) = (1, 0, 0, 0)$ *are used in the computation. (a),(c)* $\Delta t = 10^{-3}$*, (b),(d),*$\Delta t = 10^{-4}$

the solution in the smooth regions, but may fail near the cusps, with the result that error can increase dramatically in jumps. This behavior is illustrated in Fig. 2. For $m_1 = 10^{-3}$, $m_2 = 1$, a fixed stepsize of about 10^{-4} succeeds to resolve the motion near cusps. When a stepsize of 10^{-3} is used, however, the results are instability in the energy and poor resolution (especially on long time intervals). The remarkable stability of energy observed for the smaller value of Δt is a hallmark of symplectic (also time-reversible) methods and is partly explained by the "backward error analysis" of symplectic methods (see [10], [17]). The cusp points occur where $\alpha = \theta_1 - \theta_2 = 0$. At these points, in the case of $m_1 << m_2$, the vector field is nearly singular, so we conclude that the norm of the vector field is large in their vicinity.

For $m_1 = 10^{-5}$ we were unable to integrate the double pendulum with stepsizes larger than about 10^{-6}. The fixed stepsize method is extremely wasteful in terms of computation, since very large stepsizes are feasible in the smooth regions.

The results of integrating the reparameterized equations for $m_1 = 10^{-5}$ on the time interval $[0, 50]$ are summarized in Fig. 3. The scheme places many more points in the neighborhood of the turning points, but uses large timesteps on the smooth segments. We incorporated a stepsize minimum of $\Delta t_{\min} = 10^{-7}$ to restrict the smallest steps taken in the vicinity of the cusp points. About $380,000$ steps of integration were needed for this problem which would have required approximately $50,000,000$ fixed steps for similar accuracy.

4. Semi-explicit integration and the Adaptive Verlet method. In this section, we turn our attention to the mechanical system with separated Hamiltonian.

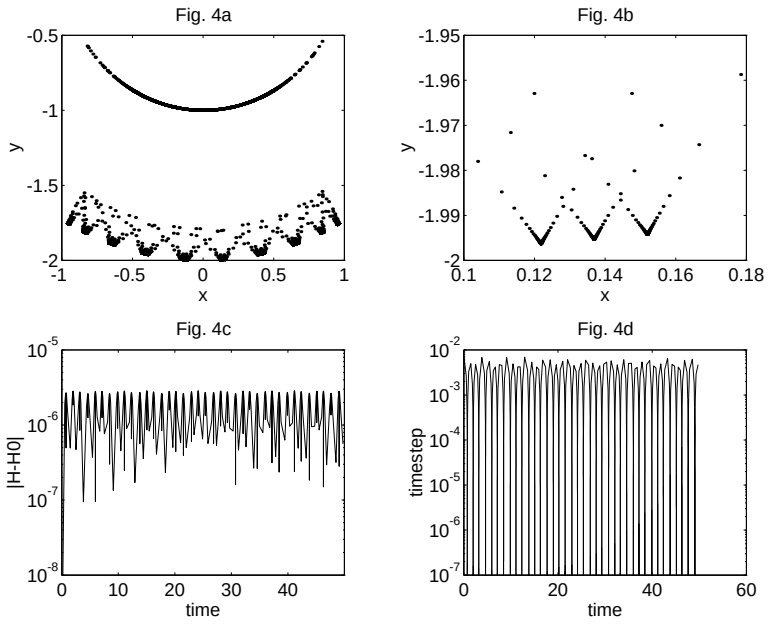

FIG. 3. *The implicit midpoint scheme with the normalized vector field for the double pendulum problem.* $m_1 = 10^{-5}$, $t_f = 50$, $\Delta s = 0.01$, *and* $(\theta_1^0, \theta_2^0, \dot{\theta_1}^0, \dot{\theta_2}^0) = (1,0,0,0)$ *are used in the computation.*

The modified equations of motion (1.3)-(1.4) reparameterized in time are

$$\frac{dq}{ds} = \frac{1}{\rho} M^{-1} p, \tag{4.7}$$

$$\frac{dp}{ds} = -\frac{1}{\rho} \nabla V(q), \tag{4.8}$$

where $\rho = R(q,p)$. The system is no longer solvable by the standard Verlet method.

The second order Lobatto IIIa-b partitioned Runge-Kutta formula [8] can be viewed as a generalization of the Verlet method. Applied to (4.7)-(4.8), the equations are (with $S = 1/R$)

$$q_{n+1} = q_n + \frac{\Delta s}{2}(S(q_n, p_{n+\frac{1}{2}}) + S(q_{n+1}, p_{n+\frac{1}{2}}))M^{-1} p_{n+\frac{1}{2}}, \tag{4.9}$$

$$p_{n+\frac{1}{2}} = p_{n-\frac{1}{2}} - \frac{\Delta s}{2}(S(q_n, p_{n+\frac{1}{2}}) + S(q_n, p_{n-\frac{1}{2}}))\nabla V(q_n). \tag{4.10}$$

For starting (and to view the scheme as a map of phase space), one may also replace (4.10) by the two steps

$$p_{n+\frac{1}{2}} = p_n - \frac{\Delta s}{2} S(q_n, p_{n+\frac{1}{2}}) \nabla V(q_n),$$

$$p_{n+1} = p_{n+\frac{1}{2}} - \frac{\Delta s}{2} S(q_{n+1}, p_{n+\frac{1}{2}}) \nabla V(q_{n+1}).$$

This discretization has the following important features [8]: (i) it reduces to Verlet for $R = 1$, (ii) it is time-reversible, (iii) it is symplectic if the problem is Hamiltonian

(i.e. if $R = R(H(q,p))$), and (iv) it preserves the angular momentum. (Higher order Lobatto pairs retain these features, but we restrict ourselves to the second order method in this article.)

Equations (4.9)-(4.10) are implicit, requiring the solution of a nonlinear system at each step, but the fact that R is scalar can be used to develop a relatively efficient Newton solver based on rank-one updates. However, still more efficient schemes are possible.

4.1. Differentiating the control. In this subsection, we describe an approach based on introducing the stepsize control as a new variable with its own differential equation. This leads, after discretization, to an algorithm requiring the evaluation of the Hessian of the potential energy function—or, in a finite difference approximation, two force evaluations per step. In the next subsection we will see that this scheme can be further improved.

Differentiating the equation $\rho = R(q,p)$ with respect to the reparameterized time s yields

$$\begin{aligned} \frac{d}{ds}\rho &= (\nabla_q R)^t \frac{d}{ds} q + (\nabla_p R)^t \frac{d}{ds} p \\ &= \frac{1}{R(q,p)} \left[(\nabla_q R)^t M^{-1} p - (\nabla_p R)^t \nabla_q V \right]. \end{aligned}$$

The idea is then to treat the coupled system in (q,p,ρ). We will illustrate for the choice

$$R(q,p) = (p^t M^{-2} p + \|\nabla_q V\|^2)^{\frac{1}{2}}.$$

(A similar scheme is obtained if upper and lower bounds are built-in to R as described above.)

Since $\nabla_p R = \frac{1}{R} M^{-2} p$ and $\nabla_q R = \frac{1}{R} V'' \nabla_q V$,

$$\frac{d}{ds}\rho = g(q,p) \equiv \frac{1}{R(q,p)^2} \left[p^t M^{-1} V'' \nabla V - p^t M^{-2} \nabla_q V \right].$$

A discretization for the resulting coupled system is obtained by partitioning the variables as q and (p,ρ) and using the second order Lobatto IIIa-b pair:

$$q_{n+1} = q_n + \frac{\Delta s}{\rho_{n+\frac{1}{2}}} p_{n+\frac{1}{2}} \tag{4.11}$$

$$\rho_{n+\frac{1}{2}} = \rho_{n-\frac{1}{2}} + \frac{\Delta s}{2} (g(q_n, p_{n-\frac{1}{2}}) + g(q_n, p_{n+\frac{1}{2}})) \tag{4.12}$$

$$p_{n+\frac{1}{2}} = p_{n-\frac{1}{2}} - \frac{\Delta s}{2} \nabla V(q_n) \left(\frac{1}{\rho_{n+\frac{1}{2}}} + \frac{1}{\rho_{n-\frac{1}{2}}} \right) \tag{4.13}$$

$$t_{n+1} = t_n + \frac{\Delta s}{\rho_{n+\frac{1}{2}}} \tag{4.14}$$

(4.12) can be rewritten as

$$\rho_{n+\frac{1}{2}} = a + \frac{\Delta s}{2} \cdot \frac{p^t_{n+\frac{1}{2}} b}{p^t_{n+\frac{1}{2}} M^{-2} p_{n+\frac{1}{2}} + c}$$

where

$$\begin{aligned} a &= \rho_{n-\frac{1}{2}} + \frac{\Delta s}{2} g(q_n, p_{n-\frac{1}{2}}) \\ b &= M^{-1}(V''(q_n) - M^{-1})\nabla V(q_n) \\ c &= \|\nabla V(q_n)\|^2 \end{aligned}$$

Then we get

$$(\rho_{n+\frac{1}{2}} - a)(p^t_{n+\frac{1}{2}} M^{-2} p_{n+\frac{1}{2}} + c) = \frac{\Delta s}{2} p^t_{n+\frac{1}{2}} b,$$

or, after multiplying by $\rho^2_{n+\frac{1}{2}}$,

$$(\rho_{n+\frac{1}{2}} - a)((\rho_{n+\frac{1}{2}} p_{n+\frac{1}{2}})^t M^{-2}(\rho_{n+\frac{1}{2}} p_{n+\frac{1}{2}}) + \rho^2_{n+\frac{1}{2}} c) = \frac{\Delta s}{2} \rho^2_{n+\frac{1}{2}} p^t_{n+\frac{1}{2}} b. \tag{4.15}$$

The observation from (4.13) that

$$\rho_{n+\frac{1}{2}} p_{n+\frac{1}{2}} = \rho_{n+\frac{1}{2}} p_{n-\frac{1}{2}} - \frac{\Delta s}{2} \nabla V(q_n) \left(1 + \frac{\rho_{n+\frac{1}{2}}}{\rho_{n-\frac{1}{2}}}\right)$$

is a linear function of $\rho_{n+\frac{1}{2}}$ allows us to conclude that (4.15) is a cubic polynomial in $\rho_{n+\frac{1}{2}}$.

For starting, we may use the formulas

$$\rho_{n+\frac{1}{2}} = \rho_n + g(q_n, p_{n+\frac{1}{2}}) \tag{4.16}$$

$$p_{n+\frac{1}{2}} = p_n - \frac{\Delta s}{2} \nabla V(q_n) \frac{1}{\rho_{n+\frac{1}{2}}}, \tag{4.17}$$

where q_0, p_0, t_0 are given and

$$\rho_0 \equiv R(q_0, p_0) = \left[p_0^t M^{-2} p_0 + \|\nabla_q V(q_0)\|^2\right]^{\frac{1}{2}}.$$

The convergence and time-reversibility of this scheme follow directly from the corresponding features of the underlying Lobatto scheme. The introduction of the new scalar variables and the fact that the scheme is no longer symplectic do not destroy the preservation of angular momentum, since, assuming only central forces, $\sum_i q^i \times \nabla_{q^i} V(q) = 0$ implies

$$\begin{aligned} \sum q^i_{n+1} \times p^i_{n+1} &= \sum q^i_{n+1} \times (p^i_{n+\frac{1}{2}} - \frac{h}{2\rho_{n+\frac{1}{2}}} \nabla_{q^i} V(q_{n+1})) \\ &= \sum q^i_{n+1} \times p^i_{n+\frac{1}{2}} \\ &= \sum (q^i_n + \frac{h}{\rho_{n+\frac{1}{2}}} p^i_{n+\frac{1}{2}}) \times p^i_{n+\frac{1}{2}} \\ &= \sum q^i_n \times (p^i_n - \frac{h}{2\rho_{n+\frac{1}{2}}} \nabla_{q^i} V(q_n)) \\ &= \sum q^i_n \times p^i_n \end{aligned}$$

In our experiments, we did not use precisely the method described here, but instead replaced (4.12) by the slightly different midpoint formula

$$\rho_{n+\frac{1}{2}} = \rho_{n-\frac{1}{2}} + \Delta s g(q_n, \frac{p_{n-\frac{1}{2}} + p_{n+\frac{1}{2}}}{2}).$$

The resulting scheme has the same convergence order (two) and the same (linearized) stability as (4.11)-(4.14), and we observed no evident degradation of performance for the cases we looked at.

In many cases, the computation of the Hessian matrix $V''(q)$ will be an intolerable expense. In these situations, we suggest using the approximation

$$V''(q_n)\nabla V(q_n) \approx \frac{1}{\epsilon}\left[\nabla V(q_n + \epsilon \nabla V(q_n)) - \nabla V(q_n)\right] \tag{4.18}$$

for some appropriately chosen ϵ. This modification changes only the definition of the time reparameterization and not the phase space dynamics. It requires two computations of the forces (at each time step). It may be useful for efficient implementation to observe that these forces are computed at two very close points in configuration space; this means that if the forces are evaluated based on lists of nearby interacting particles, the same list can be used for both calculations.

4.2. A coupled differential-algebraic system. Our preferred approach is to view the reparameterized equations

$$\begin{aligned} \frac{dq}{ds} &= \frac{1}{\rho}\nabla M^{-1} p, \\ \frac{dp}{ds} &= -\frac{1}{\rho}\nabla V(q), \\ \rho &= R(q,p) \end{aligned}$$

as a coupled differential-algebraic (DAE) system [2]. The method of the previous section can be viewed as a regularization based on differentiation of the constraints, and there is a potential for drift effects to degrade the numerical results in long time interval integration. Since long time interval simulations are precisely the applications where time-reversible methods can be expected to make a substantial difference, it may be important to correct this situation. Moreover, we would like to find a method that does not require computation of the Hessian matrix or more than one force evaluation per step.

For these reasons, we propose instead the following direct discretization of the coupled DAEs:

$$q_{n+1} = q_n + \frac{\Delta s}{\rho_{n+\frac{1}{2}}} M^{-1} p_{n+\frac{1}{2}}, \tag{4.19}$$

$$p_{n+\frac{1}{2}} = p_{n-\frac{1}{2}} - \frac{\Delta s}{2}\nabla V(q_n)\left(\frac{1}{\rho_{n-\frac{1}{2}}} + \frac{1}{\rho_{n+\frac{1}{2}}}\right), \tag{4.20}$$

$$\rho_{n+\frac{1}{2}} + \rho_{n-\frac{1}{2}} = R(q_n, p_{n+\frac{1}{2}}) + R(q_n, p_{n-\frac{1}{2}}) \tag{4.21}$$

$$t_{n+1} = t_n + \frac{\Delta s}{\rho_{n+\frac{1}{2}}}. \tag{4.22}$$

This method requires only a single evaluation of $-\nabla V$ at each step.

As for the scheme derived above based on differentiating the control, we can reduce the implicitness to a single scalar equation for $\rho_{n+\frac{1}{2}}$.

$$(\rho_{n+\frac{1}{2}} + \rho_{n-\frac{1}{2}} - R(q_n, p_{n-\frac{1}{2}}))^2 = R(q_n, p_{n+\frac{1}{2}})^2. \tag{4.23}$$

Since, for normalized dynamics,

$$R(q_n, p_{n+\frac{1}{2}})^2 = p_{n+\frac{1}{2}}^t M^{-2} p_{n+\frac{1}{2}} + \|\nabla V(q_n)\|^2,$$

it is easily seen that, after multiplying both sides of (4.23) by $\rho_{n+\frac{1}{2}}^2$, we are left with a quartic polynomial in $\rho_{n+\frac{1}{2}}$. In the more general situation of an arbitrary parameterization R, we would still obtain only a scalar nonlinear equation to solve for ρ.

For the particular situation $R = R(q)$, the computation of $\rho_{n+\frac{1}{2}}$ becomes completely explicit:

$$\rho_{n+\frac{1}{2}} = 2R(q_n) - \rho_{n-\frac{1}{2}}$$

(If R depends only on p, one can simply reverse the roles of p and q in the staggered discretization to develop an explicit method.)

The discretization (4.19)-(4.21) is an index-1 differential-algebraic integrator [2], but not of a standard form. It is easily seen to be second order accurate. We analyzed the linearized stability of the scheme to confirm the boundedness and convergence of the iteration under standard assumptions (smoothness of the vector field and boundedness of the exact solution). In particular, a condition for the stability analysis to go through is that ρ remains strictly bounded away from zero along the exact solution of interest.

By an argument precisely analogous to that given in §4.1, it is easily seen that the differential-algebraic method conserves the angular momentum. The method is clearly time-symmetric.

Now set $\Delta t_n = \frac{\Delta s}{\rho_{n+\frac{1}{2}}}$. Solving (4.19) for $p_{n+\frac{1}{2}}$ and substituting in (4.20), we obtain:

$$\begin{aligned} M\frac{q_{n+1} - q_n}{\Delta t_n} &= p_{n+\frac{1}{2}}, \\ M\frac{q_{n+1} - q_n}{\Delta t_n} &= M\frac{q_n - q_{n-1}}{\Delta t_{n-1}} - \frac{\Delta t_{n-1} + \Delta t_n}{2}\nabla V(q_n). \end{aligned}$$

Thus we can view the method as a traditional variable stepsize version of the Störmer rule.

For starting the differential-algebraic scheme from given values (q_0, p_0, ρ_0), one could employ the differentiated constraint approach of the previous section. We have instead used the following starting step with good success:

$$\begin{aligned} q_1 &= q_0 + \frac{\Delta s}{\rho_{\frac{1}{2}}} M^{-1} p_{\frac{1}{2}} \\ p_{\frac{1}{2}} &= p_0 - \frac{\Delta s}{2\rho_{\frac{1}{2}}}\nabla V(q_0) \\ \rho_{\frac{1}{2}} &= R(q_0, p_{\frac{1}{2}}). \end{aligned}$$

5. Numerical Experiments. In this section we give several numerical experiments using the new schemes. In each case, we integrated the normalized vector field without any minimum stepsize control; a maximum stepsize of $\Delta t = 1$ was used. All experiments were conducted in IEEE floating point arithmetic using double precision (machine roundoff $\approx 10^{-15}$). Excellent results were also obtained for the "bond" problem (3.5).

The use of normalization in conjunction with integrating large N-body problems is not typically appropriate, since effects of separated strong contributions to the force field are unreasonably compounded in the determination of the stepsize. Outside of the well-studied gravitational or purely electrostatic N-body problem with pairwise potential $1/r$ (see [1, 13]), we are not aware of any systematic study of appropriate time transformations for numerical integration. For the small problems considered in our experiments, normalization of the vector field appears to be a suitable choice.

5.1. The Kepler Problem. The Kepler problem with Hamiltonian

$$H = \frac{1}{2}(p_1^2 + p_2^2) - \frac{1}{r}, \qquad r = \sqrt{q_1^2 + q_2^2}$$

has long been a standard benchmark for numerical integration. For low eccentricities, the orbits can be integrated without difficulty using the standard fixed-stepsize Verlet method and one recovers with good fidelity all relevant features of the flow. A notable feature is that, in contrast to standard results for numerical integration, error growth using a symplectic method such as Verlet is only linear in time.

Our goals for the variable stepsize method are to obtain a method that is robust with respect to variation of the eccentricity e and which uses small stepsizes only as orbits pass near the origin (thus improving efficiency). We also demonstrate the similar behavior of three different methods: the method based on differentiation of the control, the same method with a finite difference approximation to evaluate the Hessian, and the differential-algebraic system.

In Figure 4, we compare the behavior of the three adaptive approaches; all give very similar results in this experiment. In Figure 5, we see that the adaptive method easily outperforms the fixed stepsize method. Observe from Fig. 5a that the energy errors (maximum over the time interval) recorded for the adaptive method are essentially constant, independent of the eccentricity e. (In fact, the relative energy errors decrease slightly with increasing e.) The number of steps for various energy errors (shown in Fig. 5b) is several orders of magnitude smaller than for fixed stepsize. Fig. 5b also shows second order of convergence of the adaptive method, the same as for the fixed stepsize version.

A more difficult case is shown in Fig. 6, where we used the adaptive scheme to compute a high eccentricity ($e = 0.99999$) orbit.

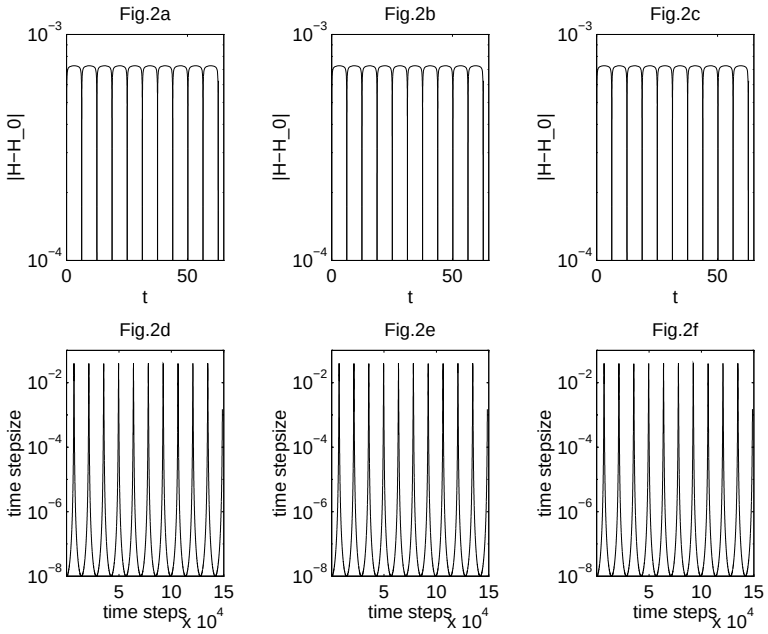

FIG. 4. *Comparison of the three adaptive methods for the Kepler problem.* $t_f = 10 \times 2\pi$, $e = 0.999$ *and* $\Delta s = 0.01$ *are used. Figs. (a) and (d) for the differentiation formula, (b) and (e) for the difference formula and (c) and (f) for the algebraic formula.*

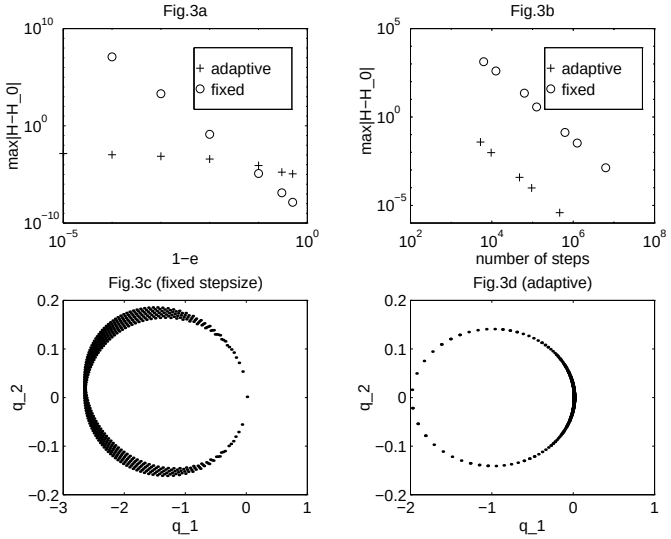

FIG. 5. *Comparison of Adaptive Verlet (differential-algebraic) method and non-adaptive Verlet methods for the Kepler problem.* $t_f = 10 \times 2\pi$ *(plotted every 100 steps). (a)* $\Delta s = 0.01$ *and* $\Delta t = 0.0001$ *are used. (b)* $e = 0.99$. *(c)* $\Delta t = 0.0001$ *and* $e = 0.99$ *are used. (d)* $\Delta s = 0.01$ *and* $e = 0.99$ *are used.*

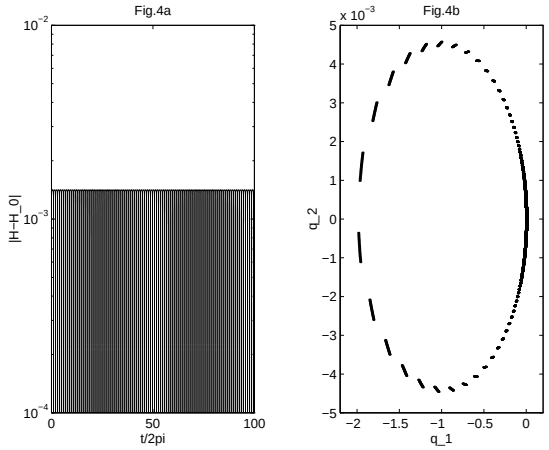

FIG. 6. *Adaptive Verlet (differential-algebraic) method for the Kepler problem.* $t_f = 100 \times 2\pi$, $\Delta s = 0.01$ *and* $e = 0.99999$ *are used in the computation. Plotted every 100 steps.*

5.2. The three-body problem. As a final example, we looked at a classical problem that is well known to present a severe challenge for standard numerical methods: the three-body problem for the gravitational (or electrostatic) interactions of three point particles. This problem has recently been treated in detail by [15] in a thorough study of the classical dynamics of Helium, since insight into the quantum mechanics of the atom can be obtained from an understanding of the bifurcations of phase space structures such as periodic orbits. There the authors point out, "Quantitative classical studies are complicated by the multidimensionality, the nonseparability, and the unbound character of the motion which is governed by singular and long-range potentials." The problem is also something of a benchmark in celestial mechanics.

As a model calculation, we sought to resolve the formation of a binary pair from a triple following a three-body near-collision. In our experiments, we did not regularize the two-body collisions as suggested in [15, 1, 13], so somewhat more efficient integration was probably possible, however, it was the three-body approach that was the chief stumbling block in our experiment. In [15], the introduction of a "fictive time" (time reparameterization) by $R = 1/(r_1 r_2)$ (where r_1 and r_2 are the separations of the two atoms from the frozen nucleus of Helium) is used to improve the behavior of the dynamical simulation.

Using unit masses and normalizing the gravitational constants, we assigned the initial positions and momenta

$$q_1 = \begin{bmatrix} 0 \\ 0 \end{bmatrix}, \quad q_2 = \begin{bmatrix} 1 \\ 0 \end{bmatrix}, \quad q_3 = \begin{bmatrix} 0 \\ 4 \end{bmatrix}, \quad p_1 = \begin{bmatrix} 0 \\ 0 \end{bmatrix}, \quad p_2 = \begin{bmatrix} 0 \\ 1 \end{bmatrix}, \quad p_3 = \begin{bmatrix} 0 \\ 0 \end{bmatrix}$$

The results of applying the adaptive method with $\Delta s = 0.5$, $\Delta s = 0.1$, and $\Delta s = 0.01$ are shown in Figs. 7a,b,c, respectively. The latter two of these integrations produce nearly identical orbits, and since the timesteps used (Figs. 7d,e,f) are an order of magnitude smaller in the third case than in the second, we conclude that with a high probability we have successfully computed the true motion.

Notice that there is a qualitative change in the behavior of the timestep after about t=3.3. At about this time, the particles are all located in a small region about

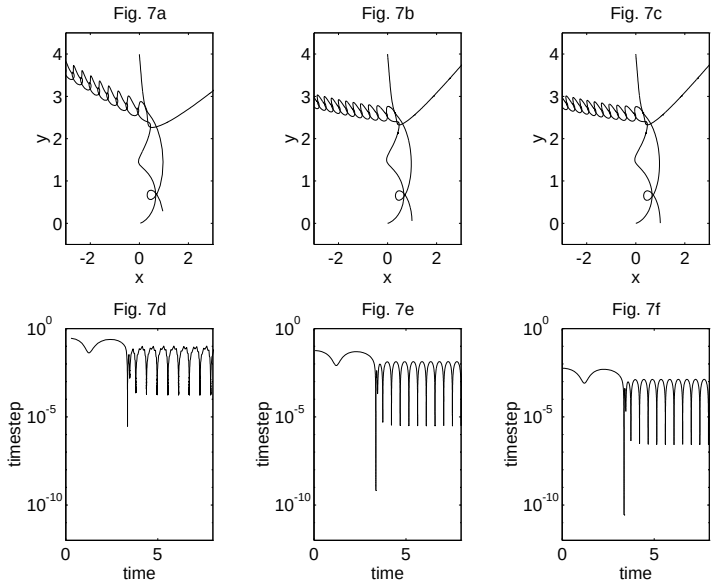

FIG. 7. *The Adaptive Verlet method on the three-body problem (a),(d)* $\Delta s = 0.5$, *(b),(e)* $\Delta s = 0.1$, *and (c),(f)* $\Delta s = 0.01$.

the point (0.25, 2.5) and the forces become very large. One particle is then ejected and the other two form a binary pair. Very small stepsizes are needed to resolve the close three-body interaction. Much larger stepsizes can be used to resolve the motion of the binary pair.

The qualitative change is also illustrated in the energy plots for the three calculations, shown in Fig. 8.

The average stepsizes used in the three variable stepsize simulations were 0.012, 0.00081 and 0.000073.

We attempted to solve the problem using fixed stepsizes $\Delta t = 10^{-4}$, $\Delta t = 10^{-5}$, and $\Delta t = 10^{-6}$. The disastrous results are shown in Figs. 9a,b,c. In all cases, the integration became completely unstable in the vicinity of the three-body approach. The energy errors, which were extremely small in the early going, rose dramatically and suddenly with this event. Fig. 10 shows a close-up of the early behavior for the case $\Delta t = 10^{-6}$.

Only for stepsizes smaller than about $\Delta t = 10^{-7}$ is the orbit successfully integrated with the fixed stepsize method, as shown in Fig. 11.

6. Conclusion. It has long been known that the use of time reparameterizations can improve the behavior of numerical methods for dynamical systems, particularly when the orbits pass in the neighborhood of singular points of the vector field. In this article, we have introduced the Adaptive Verlet method, a time-reversible integrator for reparameterized N-body problems, and shown it to be both robust and efficient in numerical experiments. One limitation of this approach is that we do not yet have a precise (quantitative) understanding of the relationship between the free parameter Δs and the accuracy of the orbit. This is the subject of current work. We are also investigating efficient higher-order adaptive time-reversible methods, and working to

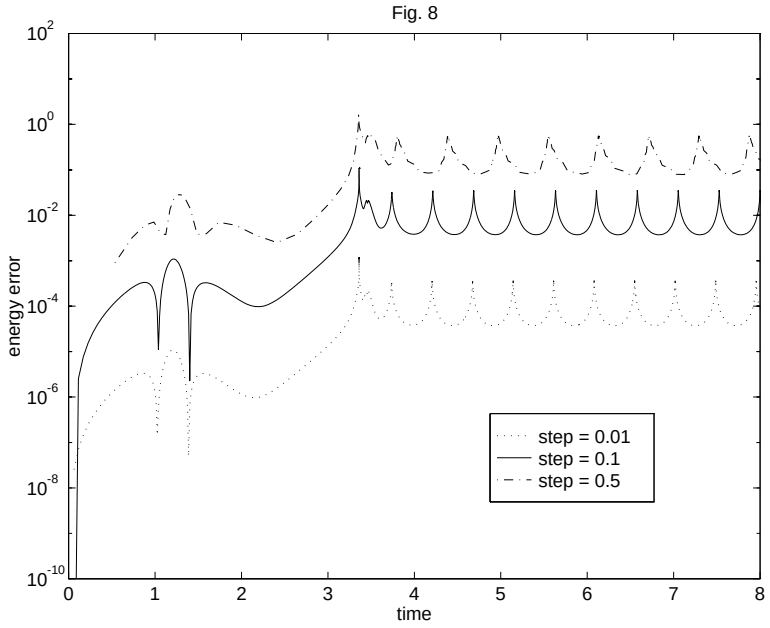

FIG. 8. *Energy errors for the Adaptive Verlet method. "Step" refers to* Δs

apply the method to constrained mechanical systems.

Acknowledgement: Bob Skeel read a preliminary draft of the article and provided useful comments.

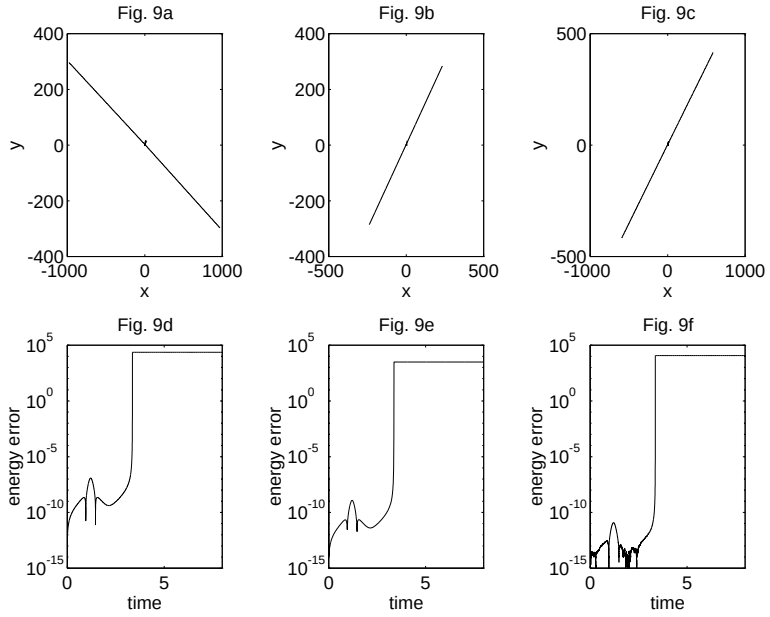

FIG. 9. *Fixed stepsize integration of the three-body problem: (a),(d)* $\Delta t = 10^{-4}$*; (b),(e)* $\Delta t = 10^{-5}$*; and (c),(f)* $\Delta t = 10^{-6}$*.*

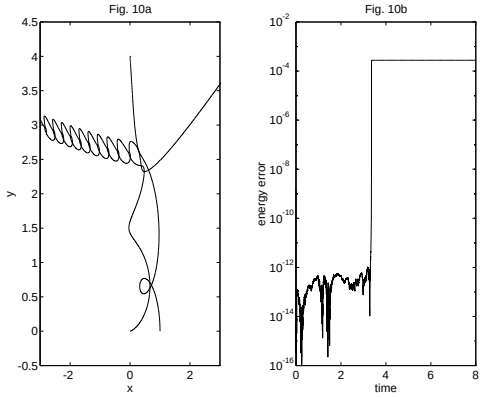

FIG. 10. *Fixed stepsize integration of the three-body problem,* $\Delta t = 10^{-6}$*, in the vicinity of (.25, 2.5).*

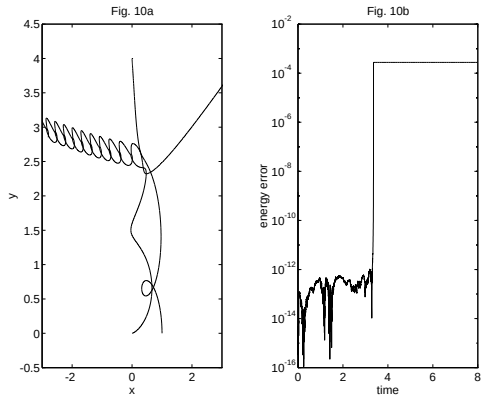

FIG. 11. *Fixed stepsize integration of the three-body problem,* $\Delta t = 10^{-7}$.

REFERENCES

[1] Aarseth, S.J., Integration methods for small N-body systems, *Predictability, Stability and Chaos in N-Body Dynamical Systems*, ed. by A. E. Roy, NATO ASI Series, Series B: Physics, North-Holland, 1991.

[2] Brenan, K., Campbell, S., and Petzold, L.R., *Numerical Solution of Initial Value Problems in Differential-Algebraic Equations*, North-Holland, New York, 1989.

[3] Calvo, M.P, and Hairer, E., Accurate long-term integration of dynamical systems, preprint, 1994.

[4] Calvo, M.P. and Sanz-Serna, J.M., The development of variable-step symplectic integrators, with application to the two-body problem, *SIAM J. Sci. Comput.*, 14, 936-952, 1993.

[5] Cooper, G.J., Stability of Runge-Kutta methods for trajectory problems, *IMA J. Num. Anal.*, 7, 1-13, 1987.

[6] Ruth, R.D., A canonical integration technique, *IEEE Trans. Nuc. Sci.*, 30, 2669, 1983.

[7] Gear, C.W. and Skeel, R.D., Does variable stepsize ruin a symplectic integrator?, *Physica D*, 60, 311-313, 1992.

[8] Sun, G., Symplectic partitioned Runge-Kutta methods, preprint, 1992.

[9] Golub, G. and Van Loan, C., *Matrix Computations*, 2nd Ed., Johns Hopkins University Press, 1989.

[10] Hairer, E., Backward error analysis of numerical integrators and symplectic methods, *Annals of Numerical Mathematics*, 1, 107-132, 1994.

[11] Hut, P., Makino, J., and Mcmillan, S., Building a better leapfrog, preprint, 1993.

[12] Leimkuhler, B., Reich, S., and Skeel, R., Numerical integration methods in molecular dynamics, preprint, 1994.

[13] Mikkola, S. and Innanen, K., A numerical experimenter's view of the few-body problem, *Predictability, Stability and Chaos in N-Body Dynamical Systems*, ed. by A. E. Roy, NATO ASI Series, Series B: Physics, North-Holland,1991.

[14] Okunbor, D., and Skeel, R., Explicit canonical methods for Hamiltonian systems, *Math. Comput.*, 59, 521-527, 1992.

[15] Richter, K., Tanner, G., and Wintgen, D., Classical mechanics of two-electron atoms, *Phys. Rev. A*, 48, 4182, 1993.

[16] Sanz-Serna, J.M., Runge-Kutta schemes for Hamiltonian systems, *BIT*, 28, 877-883, 1988.

[17] Sanz-Serna, J.M. and Calvo, M.P., *Numerical Hamiltonian Problems*, Chapman and Hall, 1994. v

[18] Shibberu, Y., Time-discretization of Hamiltonian dynamical systems, preprint, 1993.

[19] Simo, J.C., and Gonzales, O., On the stability of symplectic and energy-momentum algorithms for nonlinear Hamiltonian systems with symmetry, preprint, 1993.

[20] Skeel, R.D. and Biesiadecki, J.J., Symplectic integration with variable stepsize, *Annals of Numer. Math.*, 1, 191-198, 1994.

[21] Stoffer, D.M., Variable steps for reversible integration methods, *Computing* 55, 1-22, 1995.

[22] Wisdom, J., Some aspects of chaotic behavior in the solar system, *The Few Body Problem*, Proceedings of the 96th colloquium of the international astronomical union, Turku, Finland, 1987, M. J. Valtonen, Ed.